PPPL-1933 ① DR. 858 **PPPL-1933**

UC20-G

165 9-27-82 SA

I-5568

LINEAR AND NONLINEAR KINETIC-STABILITY STUDIES IN TOKAMAKS

By

MASTER

W.M. Tang, M.S. Chance, L. Chen,
J.A. Krommes, W.W. Lee, and G. Rewoldt

SEPTEMBER 1982

**PLASMA
PHYSICS
LABORATORY**

PPPL

**PRINCETON UNIVERSITY
PRINCETON, NEW JERSEY**

PREPARED FOR THE U.S. DEPARTMENT OF ENERGY,
UNDER CONTRACT DE-AC02-76-CHO-3073.

Printed in the United States of America.

Available from:

National Technical Information Service
U. S. Department of Commerce
5285 Port Royal Road
Springfield, Virginia 22151

Price: Printed Copy $ * ; Microfische $3.50

*PAGES	NTIS Selling Price
1-25	$5.00
26-50	$6.50
51-75	$8.00
76-100	$9.50
101-125	$11.00
126-150	$12.50
151-175	$14.00
176-200	$15.50
201-225	$17.00
226-250	$18.50
251-275	$20.00
276-300	$21.50
301-325	$23.00
326-350	$24.50
351-375	$26.00
376-400	$27.50
401-425	$29.00
426-450	$30.50
451-475	$32.00
476-500	$33.50
500-525	$35.00
526-550	$36.50
551-575	$38.00
576-600	$39.50

For documents over 600 pages, add $1.50 for each additional 25 page increment.

PPPL--1933

DE82 022200

Linear and Nonlinear Kinetic-Stability Studies in Tokamaks

W. M. Tang, M. S. Chance, L. Chen,
J. A. Krommes, W. W. Lee, and G. Rewoldt

Plasma Physics Laboratory
Princeton University
Princeton, New Jersey 08544, USA

IAEA-CN-41/D-1-3

Linear and Nonlinear Kinetic-Stability Studies in Tokamaks

This paper presents results of theoretical investigations on important linear kinetic properties of low frequency instabilities in toroidal systems and on nonlinear processes which could significantly influence their impact on anomalous transport. Analytical and numerical methods and also particle simulations have been employed to carry out these studies. In particular, the following subjects are considered: (1) linear stability analysis of kinetic instabilities for realistic tokamak equilibria and the application of such calculations to the PDX and PLT tokamak experiments including the influence of a hot beam-ion component; (2) determination of "nonlinearly saturated," statistically steady states of three interacting drift modes; and (3) gyrokinetic particle simulation of drift instabilities.

Linear Kinetic Stability Properties for Realistic Tokamak Equilibria

Since the presence of low frequency microinstabilities remains a highly plausible contributing factor to observed anomalous energy transport in tokamaks, the determination of the onset conditions for relevant modes under realistic operating situations is an important problem. In order to carry out this analysis, a numerical code has been developed to solve a set of three coupled integro-differential equations which govern the large-toroidal-mode-number ($n \gg 1$) instabilities of interest. The calculation is fully electromagnetic with the basic system of equations corresponding to comprehensive forms of the quasineutrality condition and the parallel and perpendicular components of Ampere's law. In arriving at these equations, a general form of the perturbed distribution function is used which is valid for arbitrary mode frequencies compared to the particle bounce or transit frequency and also for arbitrary perpendicular wavelengths compared to the particle gyroradius or banana width. By making use of the ballooning representation (appropriate for modes with $n \gg 1$), the linear properties can be accurately determined with a radially local (i.e., one-dimensional) analysis.[1] Collisional effects are included in the form of an energy and pitch-angle-dependent model Krook operator which reproduces the results of a Lorentz collision operator in the banana regime in the limits $\omega \ll \nu_{eff}$ and $\omega \gg \nu_{eff}$, with ν_{eff} being the effective collision frequency and ω the mode frequency. The specific mathematical form of this system of equations is quite lengthy and will not be presented here. They are given together with a detailed description of the numerical procedure employed to solve them in Ref. 2.

Since the primary goal of these studies is a realistic assessment of the kinetic stability properties under relevant experimental conditions for tokamaks, attention has accordingly been focused on two important features; namely (1) a proper interface between the stability analysis and self-consistent MHD equilibria (obtained from codes such as PEST); and (2) an appropriate treatment of the equilibrium distribution function for the hot beam-ion species which is strongly anisotropic in pitch-angle and strongly non-Maxwellian in energy, in beam-heated discharges. Regarding the first item, it is found that results from calculations using realistic equilibria can be quite different from those using the widely-adopted zero-beta model equilibrium with circular, concentric magnetic surfaces and large aspect ratio. For example, as shown in Fig. 1, a comparison between the numerical equilibrium cases and the corresponding model equilibrium cases indicates differences of around 50% in the growth rates of trapped-electron modes computed for parameters appropriate to the PDX experiment. Figure 1 also illustrates the general trend that, for realistic scenarios, kinetic instabilities are predicted to be present over a wide range of toroidal mode numbers.

In calculating the hot beam-ion response, the equilibrium distribution, $F_b(E,v_\parallel/v)$, is obtained from the BALDUR one-dimensional radial transport code [3], which also provides the equilibrium radial profiles of the densities, temperatures, and safety factor. This profile information is then used in the MHD equilibrium code to generate the corresponding numerical MHD equilibrium flux surfaces. The tokamak experimental conditions considered here are those appropriate to PLT with parallel (co-) injection and to PDX with nearly perpendicular $\{v_\parallel/v \simeq \cos(81°)\}$ injection. Figures 2 and 3 show representative forms of F_b obtained from BALDUR for these cases. Also sketched on these figures are the fundamental transit frequency resonance lines in velocity space, where $\mathrm{Re}(\omega) \equiv \omega_r \simeq \pm\,\omega_{tb}$, with ω_{tb} being the transit frequency of the beam ions. Note that the resonance lines for perpendicular injection lie in parts of velocity space where F_b is largest, while for parallel injection they fall in regions where F_b is small. This indicates that beam-ion transit-frequency resonant effects will be appreciable only in the case of perpendicular injection.

To determine the quantitative impact of the beam population on unstable modes, a systematic study was carried out for the familiar trapped-electron-drift branch. For both the PDX and PLT cases, the direct effect of the beams on these microinstabilities was found to be rather weak; i.e., the effects tend to be of the same order as the fraction of beam ions (typically, $n_b/n_e \lesssim$ 10%). This is illustrated on Fig. 1 for the PDX case. With regard to the question of how the maximum (in n or $k_\theta\rho_i$) growth rates, γ_{max}, might scale with beam power, P_b, it was found that for the PDX cases, γ_{max} decreases only slightly as P_b increases from 6.6 MW to 13.2 MW. Similar results were obtained for the PLT cases as P_b increased from 1 MW to 3 MW. Hence, substantial changes in beam power are predicted to have quite a weak effect on the drift-type microinstabilities. This appears to be consistent with recent experimental observations of the behavior of fluctuations in PDX [4].

In addition to the preceeding investigations, the general procedures described have also been applied to the kinetic analysis of high-frequency instabilities, thermonuclear alpha-particle effects, and the influence of a poloidal equilibrium electric field. Results of these ongoing studies can be briefly summarized as follows:

(1) Since velocity-space anisotropy can give rise to high frequency (ion-cyclotron frequency range) instabilities, the present low frequency gyrokinetic analysis has been appropriately generalized [5] to investigate this problem. Initial results from these calculations for PDX cases indicate that such instabilities can appear provided the beam-ion population is sufficiently large.

(2) The influence of thermonuclear alpha particles on drift-type microinstabilities has been investigated with an analytic model equilibrium distribution function of the form [6] $F_\alpha \propto n_\alpha(r)/(v^3+v_c^{\ 3})$. For the expected case of very sharply peaked n_α-profiles, a substantial stabilizing effect is found even for relatively small values of n_α/n_e.

(3) In the presence of perpendicular-injection heating, the resultant anisotropic pressure can give rise to a non-negligible equilibrium poloidal electric field. This can in turn lead to electrostatic trapping that is competitive with the usual magnetic trapping. When such effects are taken into account, preliminary results indicate that the linear growth rate of trapped-electron drift modes can be strongly modified.

Statistically Steady States of Three Interacting Drift Modes

The determination of how low frequency drift-type instabilities actually affect anomalous transport is, of course, a very important issue. It is presently believed that drift fluctuations can achieve a nonlinearly saturated steady state in which linear growth is balanced by a variety of nonlinear processes, including resonance broadening and mode coupling. Hence, a detailed understanding of these processes is required before the anomalous fluxes at saturation can be computed. Evidence from both numerical simulations and analytic theories has suggested that the saturated state is often stochastic. This implies that the phase and amplitude of the potential can wander rapidly and randomly. In order to avoid considering these complicated (and largely irrelevant) details, one is led to study a statistical description which advances in time phase-independent quantities such as the fluctuation intensity. The direct-interaction approximation (DIA) [7] is a particularly useful statistical theory, but its validity in a stochastic regime has been strongly questioned [8].

In order to test the DIA in a stochastic regime of relevance to drift wave saturation, it has been applied here to a simple system [9] consisting of three drift waves, with complex frequencies, that are quadratically coupled through the polarization and $\underline{E} \times \underline{B}$ nonlinearities. When one mode is growing while the other two are damped, it is found that this system can evolve to a saturated steady state which is stochastic. Comparison of the numerical solutions of the DIA with the "exact" numerically computed statistical dynamics arising from a Gaussian ensemble of initial conditions indicates that the predictions of the DIA are generally in reasonable agreement with the "true" values both for the modal intensities at saturation and for the two-time correlation functions. These results therefore demonstrate that the DIA does, in fact, provide satisfactory first-principles theory of the statistical dynamics of drift waves. Further studies of saturated drift-wave states with the aid of the DIA are currently in progress together with the development of related approximations which expedite the analysis of many modes in a realistic geometry [10].

Gyrokinetic Particle Simulation of Drift Instabilities

It is now widely recognized that the efficient simulation of low frequency drift-type instabilities under realistic tokamak operating conditions presents impractical demands on conventional particle codes. To remedy this difficulty, a fundamentally different type of simulation scheme has been developed which provides substantial advantages in time-step-size and in the required number of particles without sacrificing essential physics effects. Specifically, by adopting the gyrokinetic ordering (appropriate for studying low-frequency drift-type phenomena), a gyrophase-averaged form of the Vlasov-Poisson system of equations has been obtained which can be readily solved by standard particle simulation techniques [11]. The procedure here eliminates the explicit dependence on the gyromotion while still retaining finite gyroradius effects. This new scheme has been implemented into a two-and-one-half-dimensional (x,y,v_x,v_y,v_z) electrostatic code in slab geometry. For the simple case of drift instabilities driven by a density gradient in a shearless system, results from this code are given in Fig. 4 and corresponding ones from the conventional code (with full ion dynamics and the guiding-center approximation for electrons) are displayed in Fig. 5. This comparison clearly indicates very good agreement in the linear frequency and growth rate, the nonlinear frequency shift, and the saturation amplitude. Here the improvement (increase) in time-step-size is about ten-fold.

In order to simulate the more realistic steady-state type turbulence phenomena (where the background inhomogeneities are fixed in time), a multiple-scale scheme has been developed in which the long plasma equilibrium scale lengths are separated from the short scale lengths of the perturbations. Results from this modified gyrokinetic code indicate that the dominant saturation mechanisms are associated with the nonlinear $\underline{E} \times \underline{B}$ effects of the ions and electrons and with the nonlinear ion polarization drifts. In the saturated state, the spectral density of the fluctuations is broadly peaked at small k (wavenumber), and the corresponding frequency spectra has the property that the frequency spread is of the same order as the frequency, i.e., $\Delta\omega_k/\omega_k = O(1)$. Test particle measurements indicate that the diffusion is Bohm-like at this stage. In addition, a continuous exchange of energy between the different modes as well as between the particles and the waves has been observed. The fact that the results here exhibit some key properties similar to experimentally observed drift-wave phenomena should serve to motivate continued investigations of this type. In addition, the improved efficiency demonstrated by these simulations provide encouragement for developing more ambitious gyrokinetic schemes involving toroidal geometry and finite beta effects in three dimensions.

Acknowledgment

This work was supported by U.S. Department of Energy Contract No. DE-AC02-76-CHO3073.

References

[1] Frieman, E. A., Rewoldt, G., Tang, W. M., Glasser, A. H., Phys. Fluids 23 (1980) 1750.
[2] Rewoldt, G., Tang, W. M., Chance, M. S., Phys. Fluids 25 (1982) 480.
[3] Post, D. E., Singer, C. E., McKenney, A. M., and the PPPL Transport Group, TFTR Physics Group Report No. 33 (1981); BALDUR versions BALDP01G and BALDP07A.
[4] Mazzucato, E., Crowley, T. (private communication)
[5] Chen, L., Tsai, S. T., PPPL-Report No. 1816 (1981).
[6] Gaffey, J. D., J. Plasma Phys., 16 (1976) 149.
[7] Krommes, J. A., PPPL-Report No. 1568 (1980).
[8] Molvig, K., et al., Univ. of Texas IFS Report No. 30 (1981).
[9] Terry, P., Horton, W., Phys. Fluids 25 (1982) 491.
[10] Similon, P., Ph.D. Thesis, Princeton University (1981).
[11] Lee, W. W., PPPL-Report No. 1838 (1981).

Figure Captions

Fig. 1 Growth rate, γ, and real frequency, ω_r, of the trapped-electron- drift mode as a function of toroidal mode number, n, for the PDX cases with P_b = 6.6 MW at r ≈ 25 cm. The solid lines correspond to calculations using the numerical MHD equilibrium and including the beam ions. The dashed lines correspond to the same case but with the beam ions replaced by background ions. The dash-dot lines correspond to calculations using the model MHD equilibrium with circular concentric surfaces and again with beam ions replaced by background ions.

Fig. 2 Typical equilibrium distribution function, $F_b^{\shortparallel}$, for hot beam ions with parallel (co-) injection in PLT. Here P_b= 2 MW for r ≈ 20 cm at the time when the beam is turned off.

Fig. 3 Typical equilibrium distribution function, F_b, for hot beam ions with nearly perpendicular (81°) injection in PDX. Here P_b = 6.6 MW for r ≈ 25 cm at the time when the beam is turned off.

Fig. 4 Drift instability simulation results from the gyrokinetic code.

Fig. 5 Drift instability simulation results from the conventional particle code using full ion dynamics and the guiding center approximation for electrons.

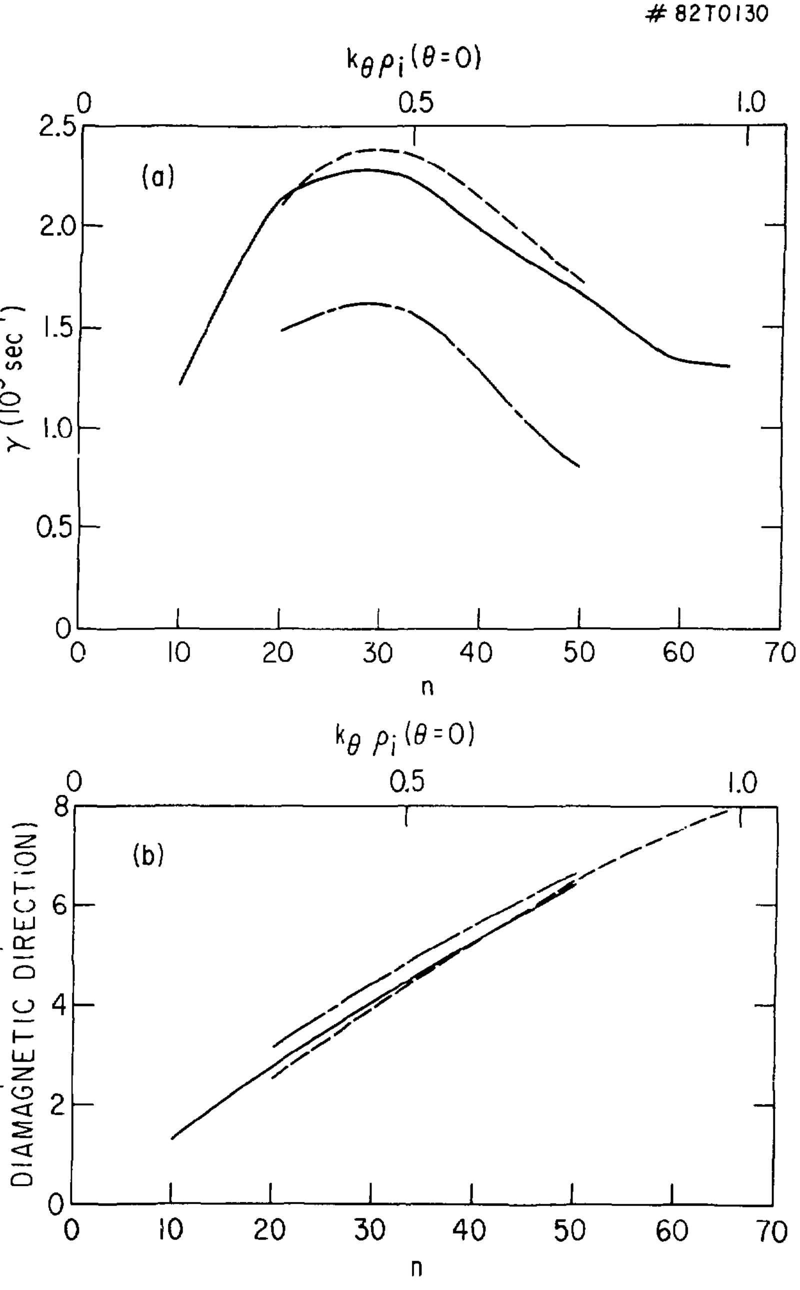
＃82T0130
$k_\theta \rho_i (\theta=0)$
0
0.5
1.0
(a)
γ (10^5 sec^{-1})
2.5
2.0
1.5
1.0
0.5
0
0
10
20
30
40
50
60
70
n
$k_\theta \rho_i (\theta=0)$
0
0.5
1.0
(b)
ω_r (10^5 sec^{-1}, ION DIAMAGNETIC DIRECTION)
8
6
4
2
0
0
10
20
30
40
50
60
70
n

Fig. 1

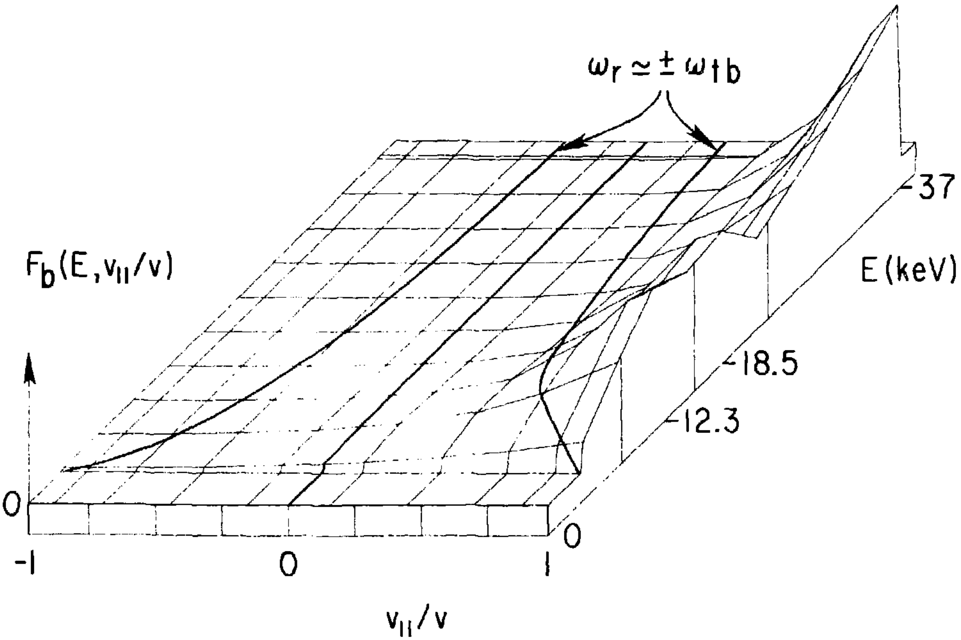
$\omega_r \simeq \pm\,\omega_{tb}$
$F_b(E, v_{\parallel}/v)$
0
-1
0
1
$v_{\parallel}/v$
0
12.3
18.5
37
E (keV)

Fig. 2

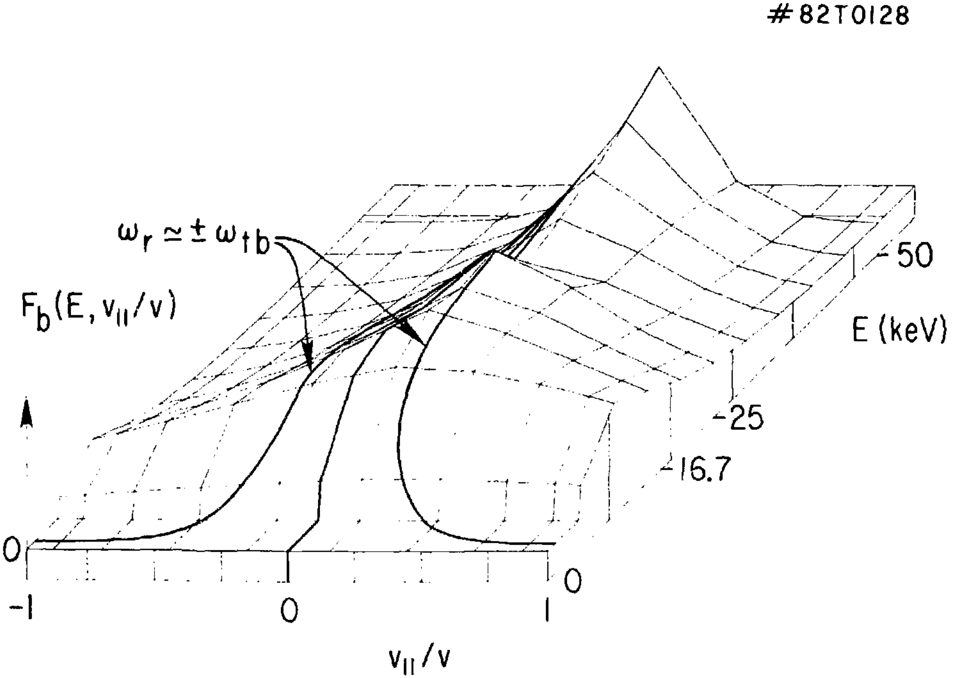
#82T0128
$\omega_r \simeq \pm \omega_{tb}$
$F_b(E, v_{\parallel}/v)$
50
E (keV)
25
16.7
0
0
-1
0
1
$v_{\parallel}/v$

Fig. 3

#82T0084

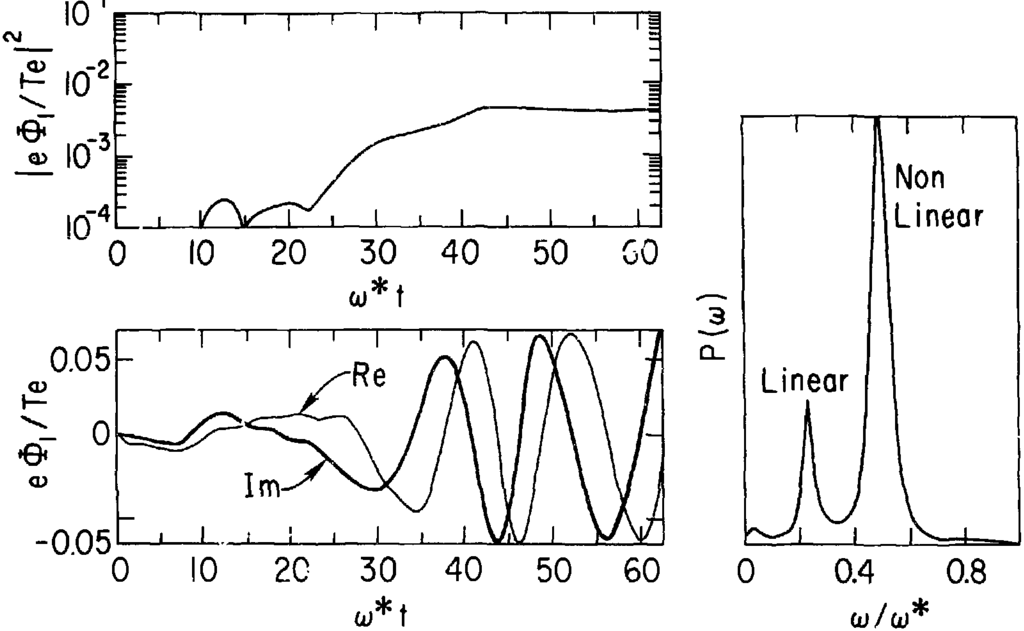

Fig. 4

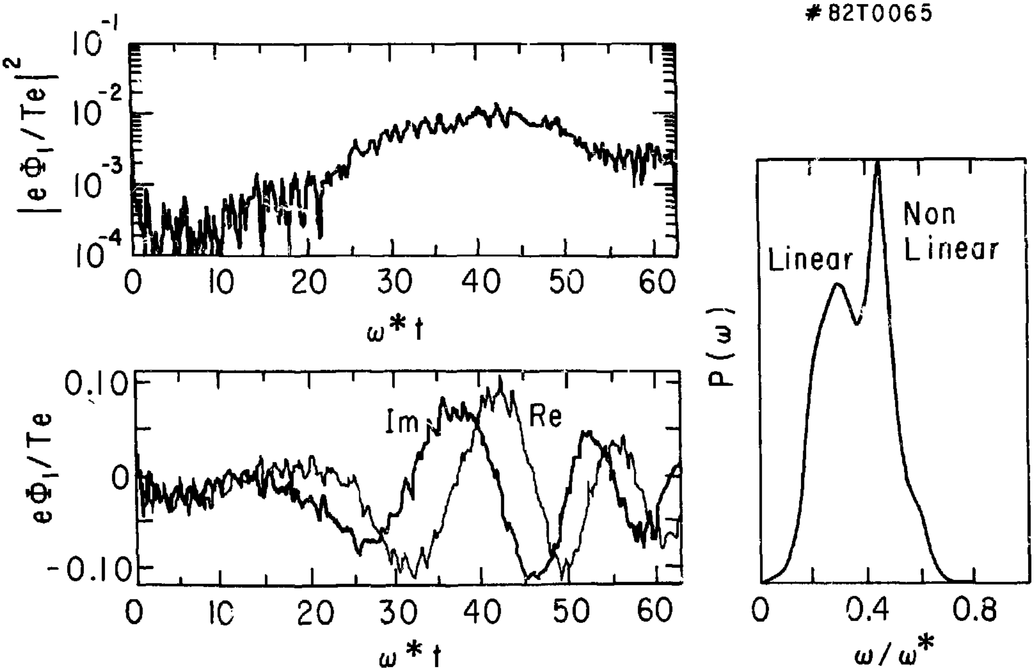
#82T0065
$|e\Phi_1/Te|^2$
10^{-1}
10^{-2}
10^{-3}
10^{-4}
0
10
20
30
40
50
60
$\omega^* t$
$e\Phi_1/Te$
0.10
0
-0.10
Im
Re
0
10
20
30
40
50
60
$\omega^* t$
$P(\omega)$
Linear
Non Linear
0
0.4
0.8
ω/ω^*

Fig. 5